Nonlocal effects in mesoscopic superconducting aluminum structures

C. Strunk, V. Bruyndoncx, V. V. Moshchalkov, C. Van Haesendonck, and Y. Bruynseraede
Laboratorium voor Vaste-Stoffysica en Magnetisme, Katholieke Universiteit Leuven, Celestijnenlaan 200 D, B-3001 Leuven, Belgium

R. Jonckheere
Interuniversity Micro-Electronics Center v.z.w., Kapeldreef 75, B-3001 Leuven, Belgium

(Received 22 July 1996)

We have measured the magnetoresistance and the magnetic phase boundary $T_c(B)$ of mesoscopic superconducting Al structures containing a loop. The structures were designed to study the nonlocal character of the superconducting condensate confined by the loop and the electrical leads connected to it. Voltage probes have been attached at several positions to monitor the superconducting transition of both the loop and the segments of the leads. Strong-coupling effects have been found to exist between the loop and the leads. At low magnetic fields, $T_c(B)$ of the lead segments reveals a pronounced oscillatory component, while the oscillation amplitude of $T_c(B)$ of the loop is significantly reduced when compared to the usual Little-Parks effect. The coupling strength is controlled by the temperature-dependent superconducting coherence length.
[S0163-1829(96)52342-8]

It has been shown that nonlocal effects may influence the electrical conductance of normal-metal submicrometer sized structures.[1] These experiments clearly demonstrated that the magnetoconductance of mesoscopic samples, which is obtained from a four terminal measurement, is also influenced by regions of the conducting structure outside the voltage probes. Due to the spatial extent of the electron wave function, all interference processes occurring within the phase coherence length L_φ contribute to the measured conductance. While the nonlocal contribution to the conductance of normal metal structures is rather small, it is enhanced in superconducting structures at temperatures above the transition temperature, where superconducting fluctuations contribute to the conduction process.[2,3]

The most pronounced nonlocal effects should be observable just *below* the superconducting transition temperature T_c, where the conductance is dominated by the presence of the superconducting condensate. In a magnetic field, parts of the sample differing in topology or dimensionality may have a difference in transition temperature, $T_c(B)$ (Ref. 4), and are expected to be coupled by the proximity effect to other parts of the structure.

Previous studies of superconductivity in mesoscopic samples[3,5] have been complicated by the presence of pronounced resistance anomalies at magnetic fields $B \lesssim 1$ mT. Very recently it was shown that these anomalies, which are related to nonmonotonic transition curves $R(T)$, can be suppressed by shielding the electrical leads against radiofrequency (rf) interference.[6] An explanation of the resistance anomalies in terms of charge imbalance around phase-slip centers created by the rf irradiation has been proposed.[6,7]

In this paper we focus on nonlocal effects in the magnetoresistance and the superconducting transition temperature of mesoscopic aluminum samples which are properly shielded from external noise. We studied square loop Al structures with a number of voltage probes connected to the current leads to monitor the superconducting transitions of the loop as well as of segments of the leads at various distances L to the loop. Strong interaction effects between the loop and the lead segments were observed, which can be tuned by varying both L and the coherence length. Our results provide experimental tests for a number of model calculations dealing with comparable structures.[8]

Samples were prepared by thermal evaporation of 99.999% pure aluminum onto oxidized silicon wafers. The patterns were defined using a bilayer polymethyl metacrylate (PMMA) resist and standard electron beam lithography methods. Scanning electron (SEM) and atomic force microscopy (AFM) confirmed the presence of a smooth aluminum surface with no major cracks or holes down to the nanometer scale. In what follows we will discuss a representative series of samples having a film thickness of 43 nm and a sheet resistance of $R_\square = 0.6\ \Omega$. The samples were prepared in a single evaporation run at room temperature to ensure an identical film thickness and no variation in the structural and electrical parameters. The Ginzburg-Landau coherence length $\xi(T)=\xi_{\rm GL}(1-T/T_{c0})^{-1/2}$ and the penetration depth $\lambda(T)=\lambda_{\rm GL}(1-T/T_{c0})^{-1/2}$ are given by $\xi_{\rm GL}=0.85(\xi_0 l_{\rm el})^{1/2}$ and $\lambda_{\rm GL}=0.66\lambda_{\rm Lo}(\xi_0/l_{\rm el})^{1/2}$. $T_{c0}=T_c(B=0)$ is the transition temperature in zero magnetic field, $\xi_0=1600$ nm the BCS coherence length, $\lambda_{\rm Lo}=15.6$ nm the London penetration depth of Al, and $l_{\rm el}$ the elastic mean-free path. The material parameters of our films are $l_{\rm el} = 16$ nm, $\xi_{\rm GL} = 0.14$ μm, and $\lambda_{\rm GL}=0.10$ μm.

The inset of Fig. 2 shows an AFM micrograph of a typical sample. It consists of strands with a width $d=0.13$ μm, interrupted by a square loop of 1-μm outer side length. The pattern enables us to measure the voltage across a 1-μm long segment of the strand on both sides of the loop as well as the voltage across the loop itself. The distance L between the inner voltage probes and the loop is varied between 0.2 and 2.0 μm. The width of the current and voltage leads is kept constant at $d=0.13$ μm to a distance of 7 μm from the outer voltage probes and the current path in order to minimize the influence of the wide parts of the contact leads on the measurement. The magnetic field is always applied perpendicular to the sample.

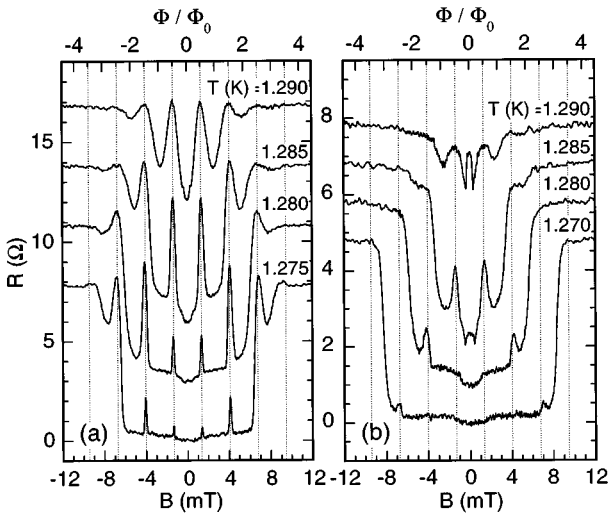

FIG. 1. Magnetoresistance of the loop (a) and a segment of the leads (b) for a typical Al sample with a 0.4-μm distance between the loop and the lead segments for various temperatures. The curves are shifted for clarity.

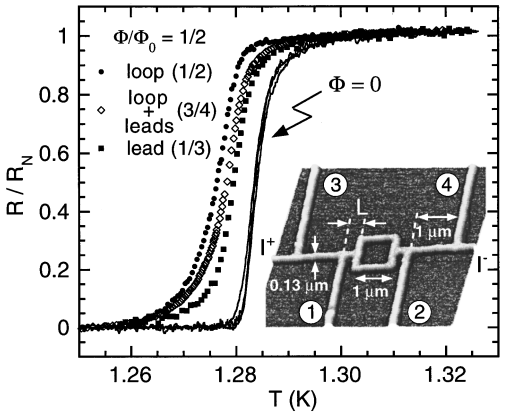

FIG. 2. Normalized resistive transitions of different segments of a sample with a 0.2-μm distance between the loop and the lead segments. The inset shows an AFM micrograph of the sample.

The ac transport measurements are performed at 27 Hz with a PAR 124A lock-in amplifier. Measuring currents I_{ac} of 50 and 100 nA rms have been used. All electrical leads are shielded by pi filters with a roll-off frequency of 1 MHz. The normal/superconducting phase boundaries, $T_c(B)$, are measured by tracing the midpoint temperature of the resistive transition with the aid of a feedback technique while slowly ramping the magnetic field. The temperature stability achieved with the feedback circuit was of the order of 0.1 mK.

As a characteristic signature of the nonlocality, an oscillatory magnetoresistance $R(B)$ of the leads segments is expected. This is confirmed by the results for $R(B)$ shown in Fig. 1. The traces in (a) are obtained while measuring across the loop (voltage contacts 1/2). The traces in (b) have been obtained for the same sample across one of the lead segments (voltage contacts 1/3), where the distance between the lead segment and the loop was $L=0.4$ μm. Not only the loop segment but also the lead segments show maxima of $R(B)$ at half-integer values of the magnetic flux, i.e., $\Phi=(n+1/2)\Phi_0$, demonstrating the nonlocal influence of the loop on the lead segments. A first evidence of the nonlocal effect of a loop connected to line samples has been reported in Ref. 3. However, this study has mainly been focused on the fluctuation regime above T_{c0} and no results on the nonlocal effects on $T_c(B)$ were provided. A small remainder of the resistance anomalies described above can still be observed in our measurements. The slight enhancement of R at low fields ($B\lesssim 1$ mT) in some of the traces of Fig. 1(b) is probably due to a small amount of remaining rf interference which is not completely suppressed by the filtering of the leads.

Next, we address the question concerning the coupling strength between the loop and the leads. In Fig. 2 the normalized $R(T)$ curves of a sample with $L=0.2$ μm are plotted. In zero magnetic field the $R(T)$ curves of all segments of the sample coincide (solid lines). For a magnetic flux enclosed by the loop of $\Phi=\Phi_0/2$ a clear shift of T_c between the loop segment (voltage contacts 1/2) and the lead segment (voltage contacts 1/3) is seen. The overall transition curve including both loop and leads (voltage contacts 3/4) is slightly broadened and coincides with the sum of the $R(T)$ curves of the subsegments. We do not observe the long-range proximity effect which has been reported by Kwong *et al.*[9] for wide Al stripes. In the latter experiment the T_c of parts of the film had been reduced by about 50 mK via reactive ion etching. Stripes with alternating etched and unetched areas showed sharp overall transition curves for lengths of the etched (i.e., normal) regions up to 50 μm. This coupling is anomalous in the sense that it does not reflect the temperature dependence of the coherence length, since the coupling extends over a distance much larger than $\xi(T)$. The origin of the anomalous proximity effect reported in Ref. 9 is still unclear.

For a more quantitative analysis of the nonlocal effect, the normal/superconducting phase boundaries of the loop and one of the lead segments were measured. $T_c(B)$ of the loop shows the classical Little-Parks (LP) oscillations (see Fig. 3) although an unexpected and pronounced increase of the oscillation amplitude $\Delta T_c(B)$ with increasing field is observed. This observation is not in agreement with previous measurements on Al microcylinders,[10] which have revealed a field-independent oscillation amplitude. Finally, as already shown in Fig. 1, the lead segments of our samples also show oscillations at low fields, which rapidly vanish when increasing the magnetic field.

To analyze the unusual field dependence of the nonlocal Little-Parks oscillations, we compare our data with the results of the Ginzburg-Landau theory for the conventional Little-Parks effect. The solid line in Fig. 3 corresponds to the calculated phase boundary of a superconducting microcylinder in an axial magnetic field:[10,11]

$$T_c(B)=T_{c0}\left\{1-\left(\frac{\xi_{GL}}{R_m}\right)^2\left[\left(\frac{\pi R_m^2 B}{\Phi_0}\right)^2(1+z^2)-2n\frac{\pi R_m^2 B}{\Phi_0}+\frac{n^2}{2z}\ln\left(\frac{1+z}{1-z}\right)\right]\right\}. \quad (1)$$

Here $R_m=(R_{max}+R_{min})/2$ is the average of the inner and outer radius of the cylinder, $d=R_{max}-R_{min}$ being the wall

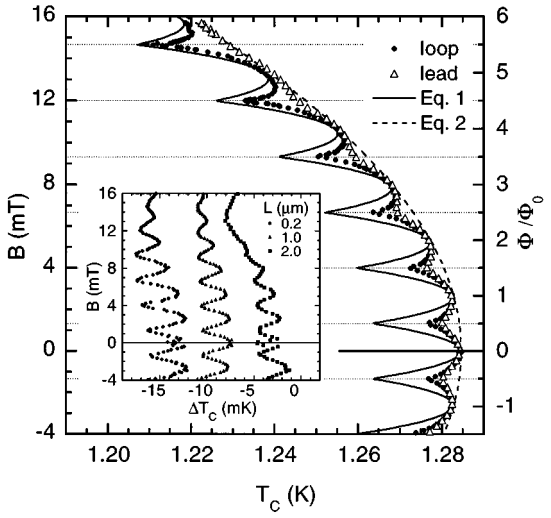

FIG. 3. Normal/superconducting phase boundaries of a loop and a lead segment ($L=0.2$ μm) as described in the text. The solid and dashed lines correspond to the theoretical phase boundaries of an isolated loop and a one-dimensional line, respectively. Inset: nonlocal Little-Parks oscillations for lead segments with varying distance to the loop L. The parabolic background depression of T_c has been subtracted.

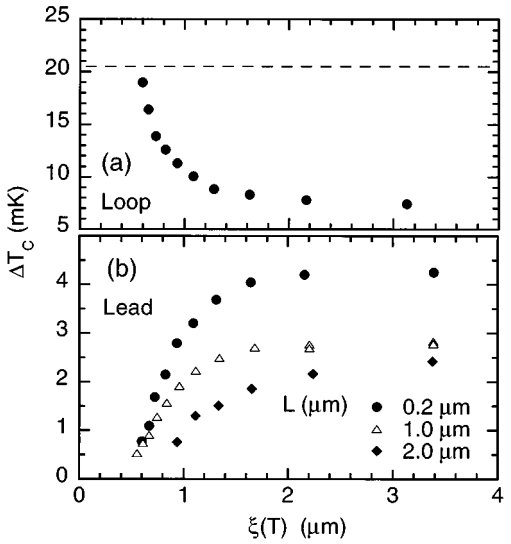

FIG. 4. Oscillation amplitude vs coherence length obtained from the phase boundaries of the loop and the lead segments shown in Fig. 3. The dashed line indicates the theoretical value of the oscillation amplitude for an isolated loop.

thickness and $z=d/2R_m$ the cylinder aspect ratio. The integer n has to be chosen to maximize $T_c(B)$ for a given value of B.

It is important to note that within the framework of the Ginzburg-Landau theory the oscillation amplitude $\Delta T_c=T_{c0}(\xi_{\mathrm{GL}}/2R_m)^2$ is field independent and not a free parameter.[11] R_m is determined from the loop area as well as from the period of the LP oscillations, while ξ_{GL} can be obtained independently from the parabolic background of $T_c(B)$ caused by the finite wall thickness d. The envelope of $T_c(B)$ for a cylinder is identical to the phase boundary $T_c(B)$ of a thin film in a parallel magnetic field:[11]

$$T_c(B)=T_{c0}\left[1-\frac{\pi^2}{3}\left(\frac{d\xi_{\mathrm{GL}}B}{\Phi_0}\right)^2\right]. \tag{2}$$

For mesoscopic samples Eqs. (1) and (2) remain valid for perpendicular fields, provided $\xi(T),\lambda(T)\gg d$.[12] This condition is always fulfilled in the temperature range under consideration. When d is known, ξ_{GL} can be determined by fitting Eq. (2) to the measured envelope of the phase boundaries. Inserting the width of the strands determined via electron microscopy, we find values for the Ginzburg-Landau coherence length which vary within a series of samples by not more than 5% and are in good agreement with the ξ_{GL} values obtained from the mean-free path l_{el}.

To further illustrate the nonlocal character of the superconducting condensate in our nanostructures, the inset of Fig. 3 shows the influence of L—the distance to the loop—on the $T_c(B)$ phase diagram of the lead segments. The oscillation amplitude of $T_c(B)$ decreases with increasing field until it vanishes in the experimental background noise. When increasing the distance between the measured lead segment and the loop, the oscillations gradually disappear at smaller fields. In order to better resolve these relatively small oscillations in the lead segments, we have subtracted the monotonic background described by Eq. (2) from the measured $T_c(B)$ curves. In some traces a small low-field suppression of T_c is present for $B\leqslant 1$ mT, corresponding to the low-field anomalies in $R(B)$ (see Fig. 1) which are probably induced by residual rf radiation.

For a quantitative determination of the magnetic field and L dependence of the oscillation amplitude ΔT_c we have exploited the fact that at the phase boundary the magnetic field B and $\xi(T)$ are related by $1/\xi(T)=(\pi dB)/(\sqrt{3}\Phi_0)$ [which is Eq. (2) rephrased in terms of $B_c(T)$ rather than $T_c(B)$]. When increasing the magnetic field, the background suppression of T_c results in a decrease of $\xi(T)$. In Fig. 4 the oscillation amplitudes ΔT_c for the loop and lead segments with different L are plotted as a function of $\xi(T)$. Note the different scales for the ΔT_c axes. Below $\xi(T)\simeq 2$ μm, ΔT_c of the loop increases with decreasing $\xi(T)$ [see Fig. 4(a)]. The dashed line corresponds to the theoretical oscillation amplitude obtained for an isolated loop with the same ξ_{GL} and d (solid line in Fig. 3). In contrast, $\Delta T_c(B)$ for the lead segments decreases with decreasing $\xi(T)$ [see Fig. 4 (b)] Hence, the change of the oscillation amplitude with increasing magnetic field is directly related to the temperature-dependent coherence length. Figure 4(b) also shows the systematic decrease of ΔT_c with increasing distance L of the lead segment to the loop.

Our experiment clearly demonstrates the interesting interplay between the loop and the leads in a superconducting mesoscopic structure. While the transition temperature of an isolated loop oscillates with a constant amplitude as a function of the magnetic field, the phase boundaries $T_c(B)$ of the leads should be monotonic in the absence of the nonlocality. Connecting the loop to the leads has an effect on both of them—the oscillations in the loop are strongly damped and $T_c(B)$ of the leads reveals an oscillatory component. As inferred from the observed temperature dependence of the two effects, the nonlocality can be linked to the stiffness of the

superconducting order parameter ψ. For $\Phi \neq n\Phi_0$ the fluxoid conservation causes a reduction of T_c of the loop. For T between the transition temperatures of the isolated systems ψ is reduced in the loop when compared to its equilibrium value in the leads and far away from the loop. When $\xi(T)$ is larger than or comparable to the loop size, the depression of ψ extends into the leads. On the other hand, due to the stabilizing influence of the leads, ψ in the loop will be considerably higher than in the case of an isolated loop.

As illustrated in Fig. 4, the length scale determining the coupling strength is indeed the coherence length $\xi(T)$. The problem of a loop with attached leads has been treated theoretically in the limit of vanishing width of the strands. Fink *et al.*[8] calculated that the presence of leads indeed reduces the oscillation amplitude of $T_c(B)$ of the loop when compared to an isolated loop. However, the theory overestimates the coupling strength by assuming a single transition temperature for the whole structure. This assumption cannot hold, when the leads are much longer than $\xi(T)$. As confirmed by the data presented in Fig. 2, we find that there is a difference between the transition temperatures of the loop and the leads, though considerably smaller than inferred from the Little-Parks effect for an isolated loop. The strictly one-dimensional theory used in Ref. 8 can also not account for the observed crossover from coupled to decoupled behavior, since the decoupling is induced by the parabolic background depression of $T_c(B)$ due to the finite width of the strands. Once T_c has been sufficiently decreased by the magnetic field, $\xi(T)$ becomes smaller than the loop size resulting in a weaker coupling and the experimental phase boundaries gradually approach the behavior of the isolated systems (see Fig. 3).

In conclusion, we have found that a mesoscopic superconducting loop and the electrical leads connected to it form a strongly coupled system. The mutual nonlocal influence is due to the divergence of the coherence length near the transition temperature and is suppressed at lower temperatures. Although simple one-dimensional models cannot account for all of our observations, a qualitative interpretation in terms of a proximitylike coupling is possible.

We thank M. Van Bael for providing the AFM micrographs of the samples as well as A. López and V. Fomin for helpful discussions. This work has been supported by the Belgian National Fund for Scientific Research (NFWO), the Belgian Inter-University Attraction Poles (IUAP), and the Flemish Concerted Action (GOA) research programs.

[1] C. P. Umbach, P. Santhanam, C. Van Haesendonck, and R. A. Webb, Appl. Phys. Lett. **50**, 1289 (1987); A. Benoit, C. P. Umbach, R. B. Laibowitz, and R. A. Webb, Phys. Rev. Lett. **58**, 2343 (1987).

[2] L. I. Glazman, F. W. Hekking, and A. Zyuzin, Phys. Rev. B **46**, 9074 (1992).

[3] N. E. Israeloff, F. Yu, A. M. Goldman, and R. Boiko, Phys. Rev. Lett. **71**, 2130 (1993).

[4] C. C. Chi *et al.*, Phys. Rev. B **50**, 3487 (1994).

[5] P. Santhanam *et al.*, Phys. Rev. Lett. **66**, 2254 (1991); H. Vloeberghs *et al.*, *ibid.* **68**, 1268 (1992); J. J. Kim *et al.*, J. Phys. Condens. Matter. **6**, 7055 (1994).

[6] C. Strunk *et al.*, Phys. Rev. B **53**, 11 332 (1996).

[7] M. Park, M. S. Isaacson, and J. M. J. Parpia, Phys. Rev. Lett. **75**, 3740 (1995).

[8] H. J. Fink, A. López, and R. Maynard, Phys. Rev. B **26**, 5237 (1982); S. B. Haley and H. J. Fink, Phys. Lett. **102A**, 431 (1984).

[9] Y. K. Kwong, K. Lin, M. S. Isaacson, and J. M. Parpia, Phys. Rev. Lett. **65**, 2905 (1990).

[10] R. P. Groff and R. D. Parks, Phys. Rev. **176**, 567 (1968).

[11] M. Tinkham, Phys. Rev. **129**, 2413 (1963).

[12] V. V. Moshchalkov *et al.*, Nature (London) **373**, 319 (1995).